A novel design method for TPMS lattice structures with complex contour based on moving elements method

Xiangyu Ma
David Zhengwen Zhang (zhangzw@cqu.edu.cn)
University of Exeter https://orcid.org/0000-0002-1561-0923
Xuewei Yu
Zhihao Ren
Shenglan Mao

Research Article

Keywords: TPMS lattice structure, Complex contour, Moving elements method, Modeling method

Posted Date: March 16th, 2022

DOI: https://doi.org/10.21203/rs.3.rs-1421576/v1

A novel design method for TPMS lattice structures with complex contour based on moving elements method

Xiangyu Ma[a,b], David Z. Zhang[a,b,c,*], Xuewei Yu[d,*], Zhihao Ren[a,b], Shenglan Mao[a,b]

a State Key Laboratory of Mechanical Transmissions, Chongqing University, Chongqing, 400044, China

b Chongqing Key Laboratory of Metal Additive Manufacturing (3D Printing), Chongqing University, Chongqing, 400044, China

c College of Engineering, Mathematics and Physical Sciences, University of Exeter, North Park Road, Exeter EX4 4QF, UK

d Guangzhou Zhongwang Longteng Software Co., Ltd, Guangzhou, 510635, China

* Corresponding author. E-mail address: zhangzw@cqu.edu.cn (D.Z. Zhang), qiming1010@outlook.com (X.W. Yu).

Abstract: Over the past few decades, there have been many important achievements on the design, research and development of minimal surface lattice structures. In this work, we propose a modeling method for triply periodic minimal surfaces (TPMS) lattice structures with complex contours. This method is based on moving elements method (MEM) and mainly includes the following parts, such as dividing the model mesh, solving the iso-surface of the TPMS in the model, obtaining the TPMS lattice structure triangular surface of the model outline, integrating the interior of the model and the outline, and finally generating an STL file that can be used for additive manufacturing. Furthermore, the representative femur model, rabbit model and gear model are provided as case studies to verify the validity and correctness of the proposed modeling method. Then, this approach is compared with the distance field method in terms of modeling speed and modeling accuracy. The research results show that the modeling method proposed in this paper has certain advantages in the generation of complex model lattice structures. Moreover, this method provides technical means and simulation data for designing TPMS lattice structures with complex contour, and offers the underlying design ideas for the development and application of the excellent physical properties of TPMS lattice structures in medicine and engineering.

Key words: TPMS lattice structure; Complex contour; Moving elements method; Modeling method

1 Introduction

Benefiting from structural advantages such as lightweight, high strength [1], superior energy absorption [2-4] and shock impact [5], the periodic lattice structure with parametric design has been widely used in impact protection devices [6], aerospace [7], and body implants [8, 9]. Advanced manufacturing features of 3D printing [10-12], such as freedom design, layer-by-layer sintering and conformal manufacturing, provide a powerful tool for the fabrication of lattice structures with complex geometric topologies [12-14] and eliminate the restrictions for designers. For instance, a lightweight phase-change thermal controller structure based on lattice structure used in spacecraft is designed and manufactured with AlSi10Mg by direct metal laser melting [15]. And the mass of the lightweight structure is 60% lighter than most traditional

structures with the same dimensions. Moreover, the thermal test results that the thermal capacity of the thermal controller based on lattice structures is increased by 50%.

Minimal surfaces (also called as TPMS), are composed of infinite, non-self-intersecting, periodic surface in three principle directions, and have been easily found in nature [16, 17]. TPMS lattice structures are more similar with natural structures without excessive connection joints due to highly interconnected with high porosities, compared with the most utilized truss lattices. Therefore, TPMS lattice structures have attracted the attention of many scholars due to its excellent physical properties, such as zero-value mean curvature and mathematical definition [18-21]. And it has been proved that TPMS lattice structures have good mechanical properties compared with conventional lattice structures [22]. Additionally, the TPMS lattice structures mainly refer to the lattice structure of four basic topological configurations, such as Primitive style (P-style), Gyroid style (G-style), Diamond style (D-style) and I-Wrapped Package style (IWP-style) [23, 24]. Furthermore, hybrid conformations, graded conformations [25, 26], network-like or sheet-like structures [27] from these four conformations were also investigated in view of mechanical properties. Additionally, the electrical conductivity, thermal conductivity and decontamination properties of TPMS lattice structure have been reported successively [28-30]. For example, a finned metal foam-phase change materials based on TPMS lattice structures was designed, and its heat transfer performances were processed. The results indicated that TPMS based foams provide great promise for use in thermal energy storage systems and thermal management systems [31]. For the piezoelectric performance, P-style piezocomposite with the same volume fraction of 50% can increase output voltage by nearly 50% under compressive strains 2%-8% compared to a piezocomposite with three intersecting ceramic cuboids [29]. More importantly, it is worth noting that such polycrystalline structures of metals consisting of grains of a few nanometers in size, which resemble essentially the TPMS of Schwarz primitive diamond, provide superior thermal and mechanical stabilities than any other forms of metastable solid states known so far [32]. Moreover, the unusual two-scale single-crystal microlattice with a diamond-triply periodic minimal surface geometry (lattice constant, approximately 30 micrometers) is found in the biomineralized skeleton of the knobby starfish. Due to lattice-level structural gradients and dislocations, the damage tolerance of this hierarchical biological microlattice was enhanced, thus providing novel insights for designing multiscale-multistage novel lightweight synthetic metamaterials with unique properties [33]. In a word, TPMS has been proved to be an advanced concept for the design and application of multiscale lattice structure with special functional or physical properties. Therefore, many scholars have tried to apply the TPMS lattice structure to multi-functional components such as medical implants, lightweight structures, and integrated load-bearing or heat-dissipating structures so as to give full play to the excellent physical properties of TPMS.

To date, few researchers have tried to apply the TPMS lattice structure to the filling of complex contour structure models to meet the needs of lightweight or special performance, such as Boolean operation [34], space element mapping method [35] and Boolean operation of distance field [36]. Meanwhile, there are some drawbacks to the

existing model method for TPMS lattice structure with complex contour. The accuracy and modeling time for TPMS lattice structure with complex contour cannot be guaranteed. This work aims to provide a design method suitable for conformal lattice structures and improve the above issue. Firstly, the modeling framework of TPMS lattice structures with complex contour is proposed. Then, the evaluation of the proposed modeling method is processed in view of modeling accuracy and modeling speed. Finally, the proposed approach is used to generate TPMS lattice structure with complex contour. The results show that the proposed modeling framework can arbitrarily fill lattice structures for complex models, and has good modeling speed and accuracy.

The rest of this paper is organized as follows. In Section 2, we describe the moving elements method (MEM), especially the marching tetrahedron (MT) and marching triangle (MTR) used in this paper. In Section 3, the proposed modeling method is evaluated in views of accuracy and modeling speed. In Section 4, different gradient TPMS lattice structures are generated by the introduced modeling method. Section 5 provides the conclusions of this work.

2 Proposed Methods

Generally, the moving cube (MC), moving square (MS), MT and MTR method are collectively referred to as MEM [37, 38]. Among them, the MC and MT methods have been widely used in the field of medical image modeling and 3D reconstruction of implicit function surfaces due to their characteristic of low space complexity, low time complexity, fast operation speed and simple implementation. Since TPMS is an implicit function surface, meanwhile the moving elements is a technology of triangulating the surface, which coincides with the description method of the file format STL commonly used in additive manufacturing. Herein, the moving elements algorithm is proposed to generate TPMS lattice structure.

2.1 Marching tetrahedron method

In order to help physicians to understand the complex anatomy present in the slices clearly, the Marching cubes (MC) was proposed for the first time, which could create a polygonal representation of constant density surfaces from a 3D array of data. And MC has been the most popular method used to generate iso-density surface of volume data in computer graphics field [39]. However, it does not guarantee the surface to be topologically consistent with the data, and it creates triangulations which contain many triangles of poor aspect ratio [40]. Another drawbacks of the MC approach is lengthy looking-up table needed to be constructed, which make the method difficult to be implemented [41]. MT is a variation of marching cubes, which overcomes the shortcomings above-mentioned [42]. Compared to the MC approach, the MT method is more facile to be implemented since there are only 16 intersection patterns exist. Furthermore, the MT method can avoid the ambiguity situation. As mentioned above, the basic principle of MT is similar to that of MC. Firstly, the space is divided into tetrahedral units, and then all tetrahedral units are traversed. Then, the triangles are

gained through connecting the intersection points of the tetrahedron and the iso-surface in a certain order. Furthermore, the surface fitting is realized. And, the detailed process of modeling is presented below.

At the first step, the pre-designed space should be divided into tetrahedral elements. Herein, the rectangular parallelepiped area commonly used in the MC is selected for tetrahedral division, due to the MT approach is derived from MC. According to the sampling accuracy, the cuboid area is divided into small cubes. And its geometric dimensions (length, width, and height) are equal to the sampling accuracy. Furthermore, the cube is divided into 5 tetrahedrons using the five-division method. Therefore, the surface fitting accuracy can be controlled by the number of tetrahedral units and the average size of triangles, which were decided by the sampling accuracy.

At the second step, the value of implicit function equation of TPMS at each corner of tetrahedron is calculated. Then, vertices of tetrahedrons are classified into two categories: **(i) filled circles:** function values at all corners of the tetrahedron are larger than or equal to zero; **(ii) hollow circle**: function values at all corners of the tetrahedron are smaller than zero. Furthermore, the 4-bit binary state value of the cube is obtained, including 16 states, as shown in Fig. 1.

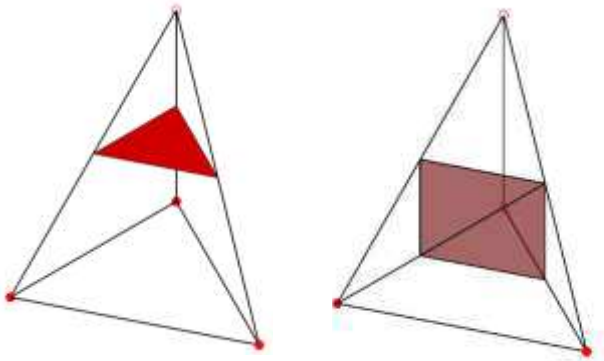

Fig. 1. Schematic diagram of the triangulation state of MT algorithm

At the third step, the equivalence triangle patch is solved through linear interpolation theory. If the state values of two points on an edge of the cube are different, the edge and the iso-surface intersect. Here, the two endpoints at different state on the edge are described by $P_1(x_1, y_1, z_1)$, $P_2(x_2, y_2, z_2)$, and the intersection point of TPMS iso-surface and cube edge is presented by $P_0(x_0, y_0, z_0)$.

$$\begin{aligned} x_0 &= x_1 + k(x_2 - x_1) \\ y_0 &= y_1 + k(y_2 - y_1) \\ z_0 &= z_1 + k(z_2 - z_1) \\ k &= \emptyset_1/(\emptyset_1 - \emptyset_2) \end{aligned} \tag{1}$$

where, $\emptyset_1$ and $\emptyset_2$ describe the function values of $P_1(x_1, y_1, z_1)$, $P_2(x_2, y_2, z_2)$ at the TPMS function. Then, the equivalence triangle patch was obtained through connecting the points.

At the final step, the fitting surface of TPMS is obtained through connecting the triangular patches solved by all tetrahedrons.

2.2 MTR method

The MTR algorithm is an iso-surface construction algorithm that reduces the dimension of the tetrahedron in the MT algorithm into a triangle. The algorithm process is the same as the MC and MT algorithms, but the MTR algorithm is different from the MT algorithm in the following points. (i) The MTR algorithm is to determine the positional relationship between the triangle and the contour. (ii) Different from MT algorithm of fitting the iso-surface, the MTR algorithm is to fit the surface inside the iso-surface. (iii) Since the MTR algorithm determines the triangle, there are a total of 8 vertex states of the triangle. If all vertices of a triangle are outside the curve, the triangle does not produce triangular patches

3 Modeling framework for TPMS lattice structure

3.1 Description of TPMS

As mentioned earlier, TPMS is a minimal surface that exhibits periodicity in three independent directions in three-dimensional space (the average curvature of any point on the surface is zero), and usually is presented as Eq. (2) in the form of an implicit surface.

$$\emptyset(r) = \sum_{k=1}^{K} A_k cos[\frac{2\pi(\boldsymbol{h}_k \cdot \boldsymbol{r})}{\lambda_k} + \boldsymbol{p}_k] \tag{2}$$

where A_k is the amplitude factor, λ_k is the trigonometric period, $\boldsymbol{r}$ is the position vector in Euclidean space, $\boldsymbol{p}_k$ is phase offset and r is independent variable.

And, the most common TPMS units, P-style, and G-style surfaces are described as Eq. (3).

$$\emptyset_{SG} = [\cos(X)\sin(Y) + \cos(Y)\sin(Z) + \cos(Z)\sin(X)]^2 = C^2$$

$$\emptyset_{NG} = \cos(X)\sin(Y) + \cos(Y)\sin(Z) + \cos(Z)\sin(X) = C$$

$$\emptyset_{NP} = \cos(X) + \cos(Y) + \cos(Z) = C$$

$$\emptyset_{SP} = [\cos(X) + \cos(Y) + \cos(Z)]^2 = C^2 \tag{3}$$

where, $X = 2\pi x/T$, $Y = 2\pi y/T$, $Z = 2\pi z/T$. T respected the period of the minimal surface. The NP, NG, SP, and SG describe the Network Primitive style, Network Gyroid style, Shell Primitive style, and Shell Gyroid style respectively.

3.2 Modeling framework

The modeling space used by the MC algorithm that can realize the modeling of TPMS lattice structure is larger than the model space to be filled, especially for thin-walled structures [43]. The larger modeling space greatly increases the number of tetrahedral that need to be processed. In this section, the modeling method for TPMS lattice structure with complex contour is introduced by combining the mentioned above algorithms.

Firstly, the tetrahedral elements in the pre-filled model are solved by the finite element meshing method, because the tetrahedral mesh obtained by the finite element meshing satisfies the principle of minimum angle maximization. Secondly, the MT algorithm is used to traverse the tetrahedral elements gained above, and then the triangular patch set of the TPMS iso-surface inside the model is achieved. In order to obtain the same TPMS lattice structure generated by the implicit function-driven, the above-mentioned TPMS iso-surface need to be sealed.

The closed operation algorithm mainly includes the following parts. Above all, triangular patches on the surface of the model are extracted through tetrahedral elements. Since a tetrahedron is composed of four triangular faces, it can be divided into two types according to the different positions of the triangular faces: (i) inner triangle: this triangular facet is shared by two tetrahedrons; (ii) surface triangle: it is unique to a tetrahedron. Herein, the basic process of obtaining the triangular facets of the specified model are presented. To ensure that the normal vector of the triangular facets is facing towards, firstly, all the tetrahedral elements are converted into four triangular in a clockwise direction. Then, the set of triangles for an object of class triangle is solved. After sorting the set of triangles, the rowIndex of all repeated triangles is gained by difference operation. Thereafter, the triangles inside the model are deleted depending on the above-mentioned rowIndex. Finally, the MTR algorithm introduced above is used to traverse each triangle surface to acquire a set of contour triangle surfaces of the lattice structure. Additionally, the duplicate vertices and triangular facets that degenerate into one point are deleted to output an STL file suitable for additive manufacturing.

3.3 Algorithm for generation of TPMS lattice structures

The modeling framework is described detail in Section 3.2, and the mathematical definition of TPMS is presented in Section 3.1. Herein, the program for the modeling of TPMS lattice structures is shown in Table 1. Firstly, the model to be processed is converted to a tetrahedral mesh. Secondly, the required minimal surface form is generated in MATLAB by Eq. (3). Then, the MT algorithm is used to obtain the internal triangular patches of the model and the triangular patches of the model surface contour, thus the lattice structure model based on a certain minimal surface is output.

Table 1 Program for the TPMS lattice structure with complex contour

Program 1
Input required model, parameters of TPMS **Output** TPMS lattice structure with contour features

Tetrahedral mesh
clear;clc;tic
model=createpde(3);
input_filename
output_filename
importGeometry(model,input_filename)
mesh=generateMesh(model,'GeometricOrder','linear','Hmax',0.5);
vertices=mesh.Nodes';
tetrahedron=mesh.Elements';
Parameters of TPMS
Cell Size=*n*;

X=@(x,y,z)2*pi/ Cell Size *x;

Y=@(x,y,z)2*pi/ Cell Size *y;

Z=@(x,y,z)2*pi/ Cell Size *z;

TPMS_style

MT algorithm

```
toc
[lat_surf.vertices,lat_surf.faces]=Surface_MT1(TPMS_G,vertices,tetrahedron);
[lat_inter.vertices,lat_inter.faces]=Internal_MT3(TPMS_G,vertices,tetrahedron);
```

Output

```
modelData.vertices=[lat_surf.vertices;lat_inter.vertices];
modelData.faces=[lat_surf.faces;lat_inter.faces+size(lat_surf.vertices,1)]
stlwrite(output_filename,modelData);
toc
```

As shown in Fig. 2, the flow chart of NG modeling with femur contour is provided based on the above algorithm. The preferred input femoral model is meshed, and the MEM method is applied to gain the internal triangular patches and contour triangular patches of the femur model, thus the femoral model based on NG lattice structure suitable for 3D printing is achieved. Moreover, NG lattice structures are used to fill the rabbit model and gear model as shown in Fig. 3 to verify the effectiveness of the modeling method. The examples show that the closed model can be filled by the TPMS lattice structure with the modeling approach based on moving element method.

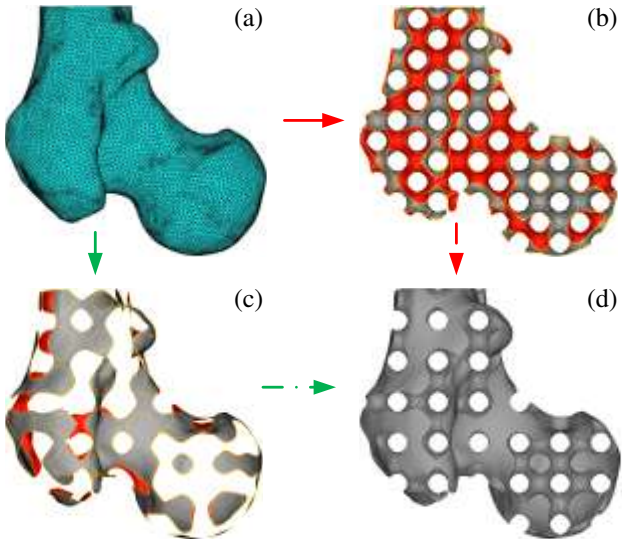

Fig. 2 Flow chart of NG modeling with femur contour: (a) Femur model; (b) NG triangular patch of femur contour; (c) NG triangular patch in femur; (d) Femoral model based on NG

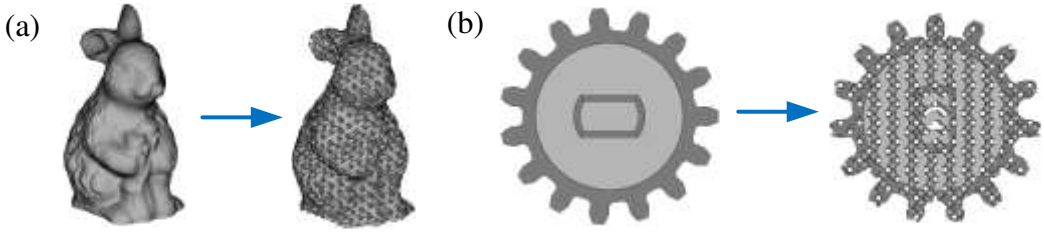

Fig. 3 Case verification: (a) Rabbit model with NG lattice structure; (b) Gear model with NG lattice structure

4 Results and Discussions

At present, the modeling methods of TPMS lattice structure mainly include four types, such as MEM, spatial element mapping method , distance field-based (DFB) modeling method [44] and surface Boolean operation algorithm. Among them, there are obvious individual difference, randomness and success rates during the Boolean and spatial element mapping method, with the distinctive experience of the operators. Nevertheless, the remaining two ways have the characteristics of simple operation and high degree of automation. Herein, the MEM and DFB modeling method are compared in this section. Depending on the modeling speed and robustness of that, the advantages and disadvantages of the two modeling methods and the scope of application are analyzed. Furthermore, the NP and NG are constructed in the cylindrical model and the complex model obtained by Boolean operations to explore the characteristics of the modeling more comprehensively.

4.1 Generation of TPMS lattice structures with complex contour

To compare and analyze the modeling speed of the above-mentioned two methods, the NP and NG lattice structure with a unit size of 4 mm are used to fill the cylindrical model and the femoral model, as shown in the following Fig. 4. The geometric dimensions of the cylinder model and the bounding box of femoral model are shown in Table 2 and Table 3, respectively. Additionally, the cylinder model equation is shown in Eq. (4) and the function expression of the cylinder in MATLAB is presented in Table 3.

$$\begin{aligned} f_{cylinder} &= \phi_1 \cap \phi_2 \\ \phi_1(x,y) &= x^2 + y^2 \le 400 \\ \phi_2(x,y) &= x^2 + y^2 \ge 196 \end{aligned} \tag{4}$$

Table 2 Geometric dimensions of the cylinder model

Cylindrical model	Inner diameter	Outer diameter	Height
Geometrical dimension (mm)	28	40	20

Table 3 Geometric dimensions of the bounding box of femoral model

Bounding box	Length	Width	Height
Geometrical dimension (mm)	19.4	18.5	12.315

Table 4 The program expression of the cylinder function

Program 2

```
WX=20; % Height of cylinder
phi_1=@(x,y,z)(z-0.5.*wx).*(z>=0)+(-0.5.*wx-z).*(z<0);
% Top and bottom equations of the cylinder
phi_2=@(x,y,z)(x.^2+y.^2-400); % Outer cylinder equation
phi_3=@(x,y,z)(-x.^2-y.^2+196); % Inner cylinder equation
cylinder=@(x, y, z )max(phi_1(x, y ,z),max(phi_2(x,y,z), phi_3(x,y,z)));
```

% Cylinder general equation

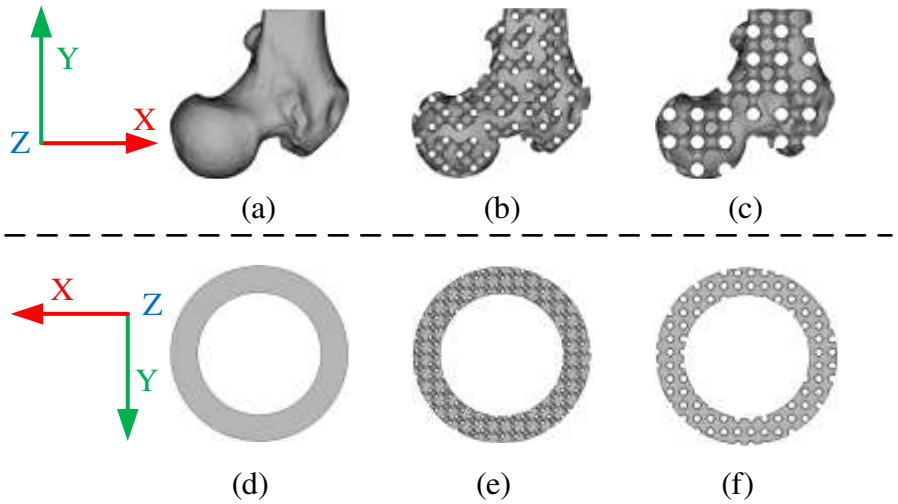

Fig. 4 (a)-(c) denote the cylinder, its NP and NG respectively
(d)-(f) denote the femur, its NP and NG respectively

4.2 Evaluation for the modeling method of lattice structure

4.2.1 Modeling speed

It is known that the modeling time is largely affected by modeling accuracy. Furthermore, it is worth noting that the obtained model still has obvious difference in surface quality with the same accuracy level, due to the fundamental difference between the DFB algorithm and the MEM in principle. Nonetheless, the lattice structures obtained by the two approaches are used to fit the curved surface with a set of triangular patches. Consequently, the accuracy of the model is positively related to the number of triangular patches with the same lattice structure. Depending on the above point of view, it is stipulated that the accuracy of the lattice structure gained by the two algorithms is considered to be consistent, when the number of triangles of the TPMS lattice structure is less than 5%, with using the same model filled by the same type.

Table 5 Comparison of modeling time

Method / Model	MEM (s)	DFB (s)
Cylinder-NP	85.997	7.197
Cylinder-NG	107.519	7.458
Femur-NP	14.738	465.065
Femur-NG	15.245	442.059

Additionally, the above-mentioned lattice structure modeling algorithms are all written in MATLAB. The operating environment of computer is AMD-4800U CPU@ 1.8GHz 4.2GHz, with the operating memory of 16GB. Furthermore, each result is run ten times and averaged to degrade the calculation error. The modeling time of various lattice structures is shown in Table 5, and the NG obtained by modeling is shown in the

Fig. 5 and Fig. 6 below.

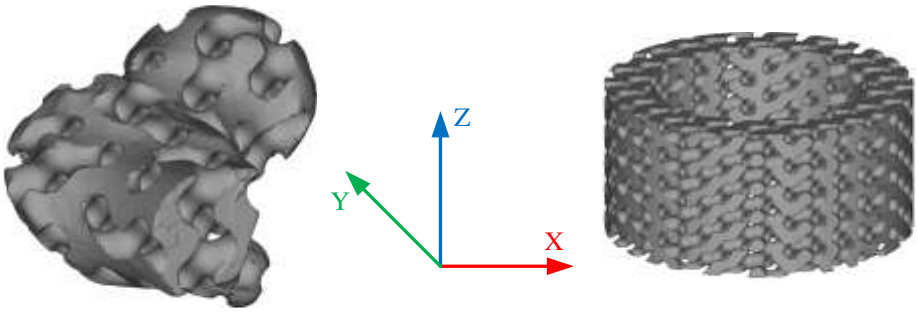

Fig. 5 The model obtained by the DFB operation

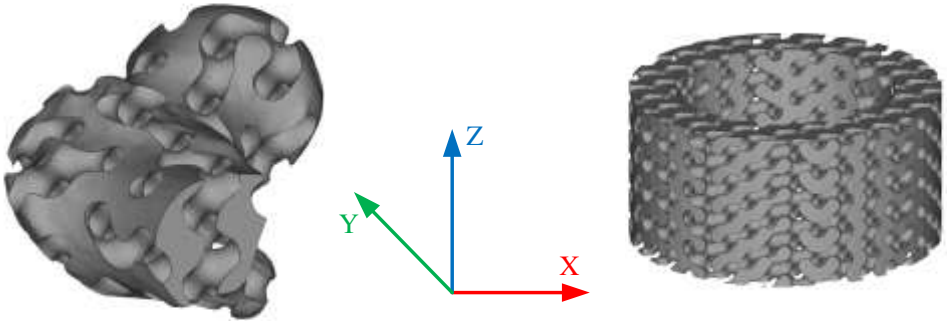

Fig. 6 Model obtained by MEM

The following conclusions can be obtained from Fig. 7: **(i) Simple geometric**: Compared with the MEM, the DFB algorithm is faster when filling the cylindrical model with the TPMS lattice, which could be explained by the reason that both TPMS and the cylindrical model can be expressed by functions. It can be clearly seen from the figure that MEM method has high modeling speed for complex such as femur model.

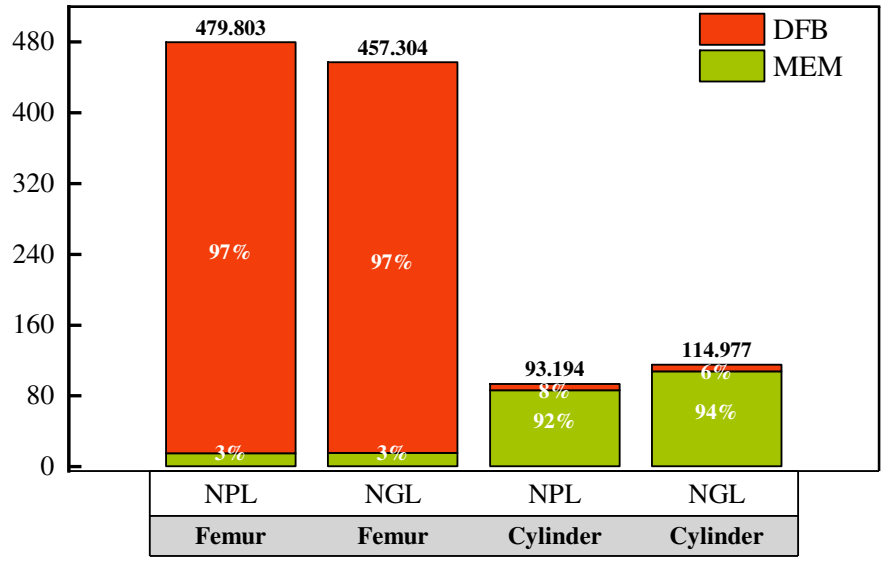

Fig. 7 Comparison of modeling time

On the other hand, DFB approach has faster modeling speed for simple models such as cylinder model. Moreover, the distance fields of TPMS and simple geometric are solved through substituting the sampling points into the equation. Furthermore, the simple TPMS lattice structure is constructed by zero iso-surface obtained by the MC

algorithm. To gain the iso-surface of the curved surface, nonetheless, the cylindrical model needs to be meshed first and then the divided tetrahedral elements are traversed during the modeling process of the moving element approach. This also explains why the MEM is significantly slower than the DFB in the modeling of simple geometry. (ii) TPMS lattice structure of complex contour: It is note that MEM only needs to traverse the tetrahedral elements inside the model and the triangles of the model outline, instead of performing operations on all the elements in the model bounding box, which contributing to reduce the time of the construction of complex contour TPMS. Nevertheless, the DFB operation method needs to calculate the shortest distance between the sampling point and the triangular patch set during modeling a complex contour TPMS, which causes a long modeling time, notwithstanding the number of sampling points could be tremendously reduced through screening of voxels. Additionally, it is found that the tetrahedral meshing time occupies large proportion throughout modeling by the MEM. Consequently, it is noteworthy that computing time could be reduced through the identical tetrahedral mesh model during filling the coequal model with different types of TPMS.

Generalize in summary, the comparison of the modeling speed during the two ways aforementioned can be acquired as the following. (i) The DFB operation method is better than moving element approach when filling the simple model. (ii) The moving element technique presents higher performance during filling a model with complex contour, compared with DFB method.

4.2.2 Robustness

In order to improve the manufacturing accuracy and processing efficiency of the construction model, the error triangles of the model should be as few as possible, and the outer contour based on the lattice structure should be consistent with the outer contour of the model. Furthermore, the error number of the triangular facets and the contour accuracy of the TPMS are determined as robustness criterion. It is note that the obvious distortion on the model surface and boundary can be effortlessly observed in the TPMS based on the DFB methodology, as shown in Fig. 5 and Fig. 6. In contrast, the TPMS lattice structure based on the moving element approach performs better in contour accuracy. Herein, the quantitative analysis of cylinder and femoral model filled by lattice structure is solved, as shown in Table 6 and Fig. 8, to compare the pros and cons of the two ways mentioned above in contour accuracy.

Table 6 Number of error triangular patches

Error type / Model	Interference housing	Overlapping triangular patch	Crossed triangular patch	Total
MEM-femur-NP	0	4	0	4
MEM-femur-NG	0	4	6	10
MEM-cylinder-NP	0	22	25	47
MEM-cylinder-NG	1	24	25	50
DFB-femur-NP	2	13	4	19

DFB-femur-NG	1	4	4	9
DFB-cylinder-NP	0	12	0	12
DFB-cylinder-NG	7	23	0	30

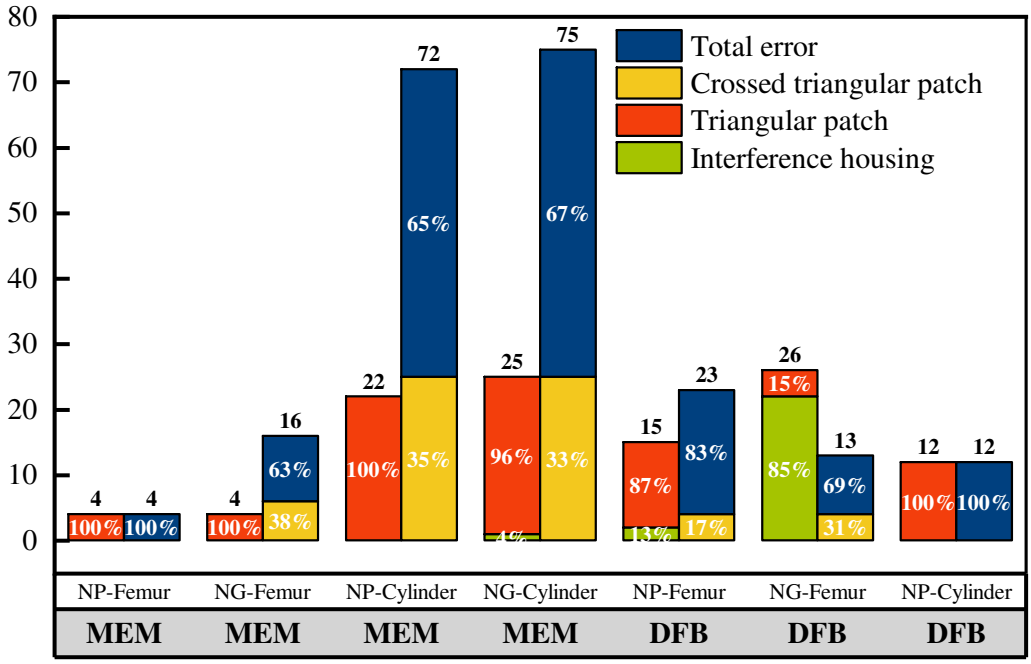

Fig. 8 Error comparison between MEM and DFB

It is intuitively gained that TPMS lattice structure with less errors in triangle patch could be constructed through the MEM and the DFB operation. Furthermore, the error triangles mentioned in the former involve overlaps and intersections, which are primarily engendered by the conversion of data format and the small intersection of tetrahedral element and surface. In addition to the overlapping triangles, there are too many erroneous triangles in the TPMS constructed by the DFB, which is mainly caused by the distortion of the algorithm. Additionally, the reasons and corrective methods for the errors of triangular faces will be explained. **(i) Overlapping triangles**: The triangular facets overlap with the adjacent triangles, mainly caused by the existence of long and narrow triangles on the surface (the acute angle is too small or the obtuse angle is too large). Therefore, it could be solved by the automatic repair of Magics Software or deleting the long and narrow triangle and connecting the adjacent triangles manually. **(ii) Cross triangular facets**: The form of this error is generally caused by the selection of data accuracy and the conversion of the data format, which can be eliminated by the automatic repair of Magics Software or redrawing the triangle manually. **(iii) Sheet**: It is the independent parts that are cut by multiple planes or curved surfaces, when the turning angle of planes or curved surfaces is larger than the slope of lattice structure. Consequently, these errors can be deleted directly.

In a word, the moving element is superior to the DFB algorithm in the accuracy of the contour, and the moving element approach is equivalent to the DFB algorithm in

the triangular patch error of the model. Therefore, MEM is superior to the DFB algorithm in terms of the robustness of modeling.

5 Conclusion and Future Work

In this paper, we propose a modeling method for obtaining the TPMS lattice structure with complex contour boundary. The MEM is used to traverse the tetrahedral elements extracted from the model, and the TPMS lattice structures with complex contour are further solved. To verify the effectiveness and superiority of this approach, some examples are introduced, and comparisons with other state-of-the-art methods are also presented. Experimental results show that our algorithm outperforms other approaches in terms of modeling time and modeling accuracy, compared with DFB modeling approach. Especially, the time used for MEM approach is reduced by 96.83% compared with DFB method when filling the NP lattice structure in the femur model. And, the time required time for MEM filling the NG lattice structure is reduced by 96.55% compared with the DFB method. Meanwhile, the number of erroneous triangular patches generated by the MEM approach is reduced by 78.95% compared to the DFB method, when filling the NP structure.

Although the presented modeling algorithm has good performance in modeling speed, adaptability and robustness, in addition, the triangular patch error of TPMS lattice structure is also less. However, there are still some problems, such as overlapping triangular patches and too many shells. In the future work, we will analyze the triangle overlap, more shell and other problems, in order to reduce the workload of manual repair errors in TPMS lattice structure manufacturing. Moreover, TPMS lattice structure model has the problem of large amount of data in lightweight applications. Therefore, the efficient design method and processing efficiency of TPMS lattice structure will be the focus of our next work. Greatly reducing the data volume of TPMS lattice structure model will provide strong support for its lightweight application.

Declaration

Funding: This work was supported by Key projects of Natural Science Foundation of Chongqing [cstc2020jcyj-zdxmX0021].
Conflicts of interest/Competing interests: The authors declare that they have no competing interests.
Availability of data and material: Not applicable
Code availability: Not applicable
Ethics approval: Not applicable
Consent to participate: Not applicable
Consent for publication: Not applicable
Authors' contributions: Xiangyu Ma, David Z. Zhang and Xuewei Yu designed the work, performed the research, and analyzed the data. Xiangyu Ma, Zhihao Ren and Shenglan Mao discussed the results and wrote the manuscript. All authors contributed to drafting and revising the manuscript.

References

[1] N.K. Thomas Tancogne-Dejean, Dirk Mohr (2019) Stiffness and Strength of Hexachiral Honeycomb-Like Metamaterials. Journal of Applied Mechanics 86. https://doi.org/10.1007/10.1115/1.4044494

[2] A. Kumar, S. Verma, J.-Y. Jeng (2020) Supportless Lattice Structures for Energy Absorption Fabricated by Fused Deposition Modeling. 3d Printing and Additive Manufacturing 7:85-96. https://doi.org/10.1007/10.1089/3dp.2019.0089

[3] C. Yang, Q.M. Li (2020) Advanced lattice material with high energy absorption based on topology optimisation. Mechanics of Materials 148. https://doi.org/10.1007/10.1016/j.mechmat.2020.103536

[4] R. Alberdi, R. Dingreville, J. Robbins, T. Walsh, B.C. White, B. Jared, B.L. Boyce (2020) Multi-morphology lattices lead to improved plastic energy absorption. Materials & Design 194. https://doi.org/10.1007/10.1016/j.matdes.2020.108883

[5] P. Tran, C. Peng (2020) Triply periodic minimal surfaces sandwich structures subjected to shock impact. Journal of Sandwich Structures & Materials 109963622090555. https://doi.org/10.1007/10.1177/1099636220905551

[6] X. Wang, C. Wang, X. Zhou, D. Wang, M. Zhang, Y. Gao, L. Wang, P. Zhang (2020) Evaluating Lattice Mechanical Properties for Lightweight Heat-Resistant Load-Bearing Structure Design. Materials 13. https://doi.org/10.1007/10.3390/ma13214786

[7] H. Zhou, X. Cao, C. Li, X. Zhang, H. Fan, H. Lei, D. Fang (2021) Design of self-supporting lattices for additive manufacturing. Journal of the Mechanics and Physics of Solids 148. https://doi.org/10.1007/10.1016/j.jmps.2021.104298

[8] S. Wang, Z.a. Shi, L. Liu, X. Zhou, L. Zhu, Y. Hao (2020) The design of Ti6Al4V Primitive surface structure with symmetrical gradient of pore size in biomimetic bone scaffold. Materials & Design 193:108830. https://doi.org/10.1007/10.1016/j.matdes.2020.108830

[9] S. Vijayavenkataraman, L.Y. Kuan, W.F. Lu (2020) 3D-printed ceramic triply periodic minimal surface structures for design of functionally graded bone implants. Materials & Design 191:108602. https://doi.org/10.1007/10.1016/j.matdes.2020.108602

[10] A. Khalil, F.E. Ahmed, N. Hilal (2021) The emerging role of 3D printing in water desalination. Sci Total Environ 790:148238. https://doi.org/10.1007/10.1016/j.scitotenv.2021.148238

[11] T.D. Ngo, A. Kashani, G. Imbalzano, K.T.Q. Nguyen, D. Hui (2018) Additive manufacturing (3D printing): A review of materials, methods, applications and challenges. Composites Part B: Engineering 143:172-196. https://doi.org/10.1007/10.1016/j.compositesb.2018.02.012

[12] M. Attaran (2017) The rise of 3-D printing: The advantages of additive manufacturing over traditional manufacturing. Business Horizons 60:677-688. https://doi.org/10.1007/10.1016/j.bushor.2017.05.011

[13] J. Song, M. Cao, L. Cai, Y. Zhou, J. Chen, S. Liu, B. Zhou, Y. Lu, J. Zhang, W. Long, L. Li (2021) 3D printed polymeric formwork for lattice cementitious composites. Journal of Building Engineering 43. https://doi.org/10.1007/10.1016/j.jobe.2021.103074

[14] C.M. Spadaccini (2019) Additive manufacturing and processing of architected materials. MRS Bulletin 44:782-788. https://doi.org/10.1007/10.1557/mrs.2019.234

[15] H. Zhou, X. Zhang, H. Zeng, H. Yang, H. Lei, X. Li, Y. Wang (2019) Lightweight structure of a phase-change thermal controller based on lattice cells manufactured by SLM. Chinese Journal of Aeronautics 32:1727-1732. https://doi.org/10.1007/10.1016/j.cja.2018.08.017

[16] L. Han, S. Che (2018) An Overview of Materials with Triply Periodic Minimal Surfaces and Related Geometry: From Biological Structures to Self-Assembled Systems. Adv Mater 30:e1705708. https://doi.org/10.1007/10.1002/adma.201705708
[17] R. Ebihara, H. Hashimoto, J. Kano, T. Fujii, S. Yoshioka (2018) Cuticle network and orientation preference of photonic crystals in the scales of the weevil Lamprocyphus augustus. J R Soc Interface 15. https://doi.org/10.1007/10.1098/rsif.2018.0360
[18] H. Montazerian, M.G.A. Mohamed, M.M. Montazeri, S. Kheiri, A.S. Milani, K. Kim, M. Hoorfar (2019) Permeability and mechanical properties of gradient porous PDMS scaffolds fabricated by 3D-printed sacrificial templates designed with minimal surfaces. Acta Biomaterialia 96:149-160. https://doi.org/10.1007/10.1016/j.actbio.2019.06.040
[19] N. Sreedhar, N. Thomas, O. Al-Ketan, R. Rowshan, H. Hernandez, R.K. Abu Al-Rub, H.A. Arafat (2018) 3D printed feed spacers based on triply periodic minimal surfaces for flux enhancement and biofouling mitigation in RO and UF. Desalination 425:12-21. https://doi.org/10.1007/10.1016/j.desal.2017.10.010
[20] N. Sathishkumar, N. Vivekanandan, L.Balamurugan, N. Arunkumar, I. Ahamed (2020) Mechanical Properties of Triply Periodic Minimal Surface based lattices made by Polyjet Printing. Materials Today: Proceedings 22:2934-2940. https://doi.org/10.1007/10.1016/j.matpr.2020.03.427
[21] R. Miralbes, D. Ranz, F.J. Pascual, D. Zouzias, M. Maza (2020) Characterization of additively manufactured triply periodic minimal surface structures under compressive loading. Mechanics of Advanced Materials and Structures. https://doi.org/10.1007/10.1080/15376494.2020.1842948
[22] M. Zhao, F. Liu, G. Fu, D.Z. Zhang, T. Zhang, H. Zhou (2018) Improved Mechanical Properties and Energy Absorption of BCC Lattice Structures with Triply Periodic Minimal Surfaces Fabricated by SLM. Materials (Basel) 11. https://doi.org/10.1007/10.3390/ma11122411
[23] M. Ouda, O. Al-Ketan, N. Sreedhar, M.I.H. Ali, R.K. Abu Al-Rub, S. Hong, H.A. Arafat (2020) Novel static mixers based on triply periodic minimal surface (TPMS) architectures. Journal of Environmental Chemical Engineering 8. https://doi.org/10.1007/10.1016/j.jece.2020.104289
[24] M. Shen, W. Qin, B. Xing, W. Zhao, S. Gao, Y. Sun, T. Jiao, Z. Zhao (2021) Mechanical properties of 3D printed ceramic cellular materials with triply periodic minimal surface architectures. Journal of the European Ceramic Society 41:1481-1489. https://doi.org/10.1007/10.1016/j.jeurceramsoc.2020.09.062
[25] M. Zhao, D.Z. Zhang, F. Liu, Z. Li, Z. Ma, Z. Ren (2020) Mechanical and energy absorption characteristics of additively manufactured functionally graded sheet lattice structures with minimal surfaces. International Journal of Mechanical Sciences 167:105262. https://doi.org/10.1007/10.1016/j.ijmecsci.2019.105262
[26] X. Ma, D.Z. Zhang, M. Zhao, J. Jiang, F. Luo, H. Zhou (2021) Mechanical and energy absorption properties of functionally graded lattice structures based on minimal curved surfaces. The International Journal of Advanced Manufacturing Technology 118:995-1008. https://doi.org/10.1007/10.1007/s00170-021-07768-y
[27] A. Alhammadi, O. Al-Ketan, K.A. Khan, M. Ali, R. Rowshan, R.K. Abu Al-Rub (2020) Microstructural characterization and thermomechanical behavior of additively manufactured AlSi10Mg sheet cellular materials. Materials Science and Engineering: A 791. https://doi.org/10.1007/10.1016/j.msea.2020.139714
[28] N. Thomas, N. Sreedhar, O. Al-Ketan, R. Rowshan, R.K. Abu Al-Rub, H. Arafat (2018) 3D printed triply periodic minimal surfaces as spacers for enhanced heat and mass transfer in membrane

distillation. Desalination 443:256-271. https://doi.org/10.1007/10.1016/j.desal.2018.06.009
[29] H. Xu, Y.M. Xie, R. Chan, S. Zhou (2020) Piezoelectric properties of triply periodic minimum surface structures. Composites Science and Technology 200:108417. https://doi.org/10.1007/10.1016/j.compscitech.2020.108417
[30] D.W. Abueidda, R.K. Abu Al-Rub, A.S. Dalaq, D.-W. Lee, K.A. Khan, I. Jasiuk (2016) Effective conductivities and elastic moduli of novel foams with triply periodic minimal surfaces. Mechanics of Materials 95:102-115. https://doi.org/10.1007/10.1016/j.mechmat.2016.01.004
[31] Z.A. Qureshi, E. Elnajjar, O. Al-Ketan, R.A. Al-Rub, S.B. Al-Omari (2021) Heat transfer performance of a finned metal foam-phase change material (FMF-PCM) system incorporating triply periodic minimal surfaces (TPMS). International Journal of Heat and Mass Transfer 170:121001. https://doi.org/10.1007/10.1016/j.ijheatmasstransfer.2021.121001
[32] Z.H.J. X. Y. Li, X. Zhou, K. Lu (2020) Constrained minimal-interface structures in polycrystalline copper with extremely fine grains. Science. https://doi.org/10.1007/10.1126/science.abe1267
[33] H.C. Ting Yang, Zian Jia, Zhifei Deng, Liuni Chen, Emily M. Peterman, James C. Weaver, Ling Li (2022) A damage-tolerant, dual-scale, single-crystalline microlattice in the knobby starfish, Protoreaster nodosus. Science 375:647–652.
[34] F. Liu, Z. Mao, P. Zhang, D.Z. Zhang, J. Jiang, Z. Ma (2018) Functionally graded porous scaffolds in multiple patterns: New design method, physical and mechanical properties. Materials & Design 160:849-860. https://doi.org/10.1007/10.1016/j.matdes.2018.09.053
[35] S. Cai, J. Xi, C.K. Chua (2012) A novel bone scaffold design approach based on shape function and all-hexahedral mesh refinement. Methods Mol Biol 868:45-55. https://doi.org/10.1007/10.1007/978-1-61779-764-4_3
[36] D.J. Yoo (2011) Porous scaffold design using the distance field and triply periodic minimal surface models. Biomaterials 32:7741-7754. https://doi.org/10.1007/10.1016/j.biomaterials.2011.07.019
[37] W.E. Lorensen (2020) History of the Marching Cubes Algorithm. IEEE Computer Graphics and Applications.
[38] E.O.P. S. L. CHAN (1998) A NEW TETRAHEDRAL TESSELATION SCHEME FOR ISOSURFACE GENERATION. Comput. & Graphics 22:83-90. https://doi.org/10.1007/10.1016/S0097-8493(97)00085-X
[39] H.E.C. William E. Lorensen (1987) MARCHING CUBES: A HIGH RESOLUTION 3D SURFACE CONSTRUCTION ALGORITHM. Computer Graphics 21. https://doi.org/10.1007/10.1145/37401.37422
[40] R.W.P. G.M. Treece, A.H. Gee (1999) Technical Section Regularised marching tetrahedra: improved iso-surface extraction. Computers & Graphics 23:583-598. https://doi.org/10.1007/10.1016/S0097-8493(99)00076-X
[41] T. Lu, F. Chen (2012) Quantitative analysis of molecular surface based on improved Marching Tetrahedra algorithm. Journal of Molecular Graphics & Modelling 38:314-323. https://doi.org/10.1007/10.1016/j.jmgm.2012.07.004
[42] E.O.P. S. L. CHAN (1998) A NEW TETRAHEDRAL TESSELATION SCHEME FOR ISOSURFACE GENERATION. Comput. & Graphics.
[43] Z.K. ZHANG Zhuangya, LI Yuesong, DUAN Mingde (2020) Porous structure method of bone scaffold based on voxel and triple cycle minimal surfaces. Computer Integrated Manufacturing

Systems 26:697-706. https://doi.org/10.1007/10.13196/j.cims.2020.03.013
[44] L.L. Yu Xuewei, Zhang Tao, Zhang Zhengwen (2021) Modeling of complex contour lattice structure based on triply periodic minimal surface and voxel distance field. Journal of Chongqing University. https://doi.org/10.1007/10.11835/j.issn.1000-582X.2021.115